中國機械工程學刊第四十五卷第五期第 435~443 頁(民國一百一十三年)
Journal of the Chinese Society of Mechanical Engineers, Vol.45, No.5, pp435~443 (2024)

Surface Finish of a Stainless Steel Using a New Ball Polishing Tool on a CNC Turning Center

Fang-Jung Shiou*, Chang-Mou Wu**, Shi-Han Hong***
and Wei-Cheng Huang***

Keywords： ball burnishing, ball polishing, lab-made polishing ball, CNC turning center, Surface roughness, STAVAX stainless mold steel.

ABSTRACT

A new ball polishing tool that can be mounted on the turret of a CNC turning center has been developed, to perform the precision surface finish of the STAVAX stainless mold steel. To simplify the conventional ball polishing with a slurry container, the lab-made polishing balls mainly composed of the NBR silicon rubber, the abrasive of aluminum oxide, and the silicon oxide have been developed and used. Five type of polishing balls with different abrasive grain sizes and concentration, from type A to type E, have been figured out, tested and fabricated. The developed polishing balls have been adopted to perform the surface finishing on the CNC turning center, to improve the surface roughness of the burnished STAVAX stainless mold steel. The effects of the number of passes using the lab-made polishing balls on the surface roughness improvement have also been investigated. According to the experimental results on the hexahedron surfaces, the polishing ball of type E, with grain size of 3 μm and concentration of 40%, has the best surface roughness improvement; and the best ball polishing passes combination were: E-C-B-A. Applying the suitable parameters of ball burnishing and ball polishing processes to the test workpiece with a keyway, the surface roughness improvement from Ra 0.21 μm to Ra 0.02 μm could be obtained. Using these suitable parameters to the workpiece with a cam profile, the improvement on the surface roughness form Ra 0.206 μm to R_a 0.03 μm could be obtained.

Paper Received July, 2024. Revised August, 2024. Accepted Ocober, 2024. Author for Correspondence: Fang-Jung Shiou.

* *Professor, Department of Mechanical Engineering, National Taiwan University of Science and Technology, Taipei, Taiwan 106335, ROC.*
email: shiou@mail.ntust.edu.tw

** *Professor, Department of Material Science and Engineering, National Taiwan University of Science and Technology, Taipei, Taiwan 106335, ROC.*
email: cmwu@mail.ntust.edu.tw

*** *Graduate Student, Department of Mechanical Engineering, National Taiwan University of Science and Technology, Taipei, Taiwan 106335, ROC.*
email: m10503211@mail.ntust.edu.tw

*** *Graduate Student, Department of Mechanical Engineering, National Taiwan University of Science and Technology, Taipei, Taiwan 106335, ROC.*
email: m10403237@mail.ntust.edu.tw

INTRODUCTION

Precision surface machining and surface finish plays an important role for some advanced industrial products, such as car components, optical components, semiconductor components, molds, and medical components, etc. To achieve the precision form accuracy and surface finish of the industrial products, different kinds of mechanical and electromechanical precision surface finishing processes, such as diamond turning, polishing, lapping, burnishing, grinding, etc. are mainly adopted (Shiou et al., 2019). The machine tools for the precision machining and surface finish can be divided into the ultraprecision machine tools with the positioning accuracy of nanometer range and the CNC machine tools with the positioning accuracy of micrometer range assisted by integrating with some specially developed tools.

The effects of magnetic field assistance on the quality of surface finish for sustainable manufacturing of ultra-precision single-point diamond turning of titanium alloys have been experimentally investigated in (Hatefi et al., 2022). The surface finishing and tool wear in single point diamond turning of chemical vapor deposited tungsten carbide hard coatings has been discussed in (Micallef et al. 2022). A review of cutting tools for ultra-precision machining has been introduced in (Ganesan et al. 2023). The ultra-precision bonnet polishing technology has been reviewed in (Wu et al. 2022). After finishing the diamond turning, the effect of parameters on surface roughness during the ultra-precision polishing of titanium alloy using bonnet polishing has been studied in (Lou et al. 2022). The theoretical and experimental investigation of material removal in semi-rigid bonnet polishing of binderless tungsten carbide has been discussed in (Wu et al. 2023).

The finishing characteristics of Inconel alloy 625 bars in ultra-precision magnetic abrasive finishing using CNC machine center have been investigated in (Bae et al. 2021). To reduce the volumetric wear of a ball polishing tool, an ultrasonic-vibration-assisted polishing process has been used in (Shiou et al. 2022). The mirror surface finishing of hardened stainless steel could be obtained by using the spherical PCD tool (Kasuriya et al. 2022). Ball burnishing of Mg alloy using a newly developed burnishing tool with on-machine force control has been presented in (Cao et al. 2019).

The precision surface finish has been implemented by using the specially designed burnishing tools on a CNC lathe (Shiou et al. 2017; Maximov et al. 2024; Takasugi et al. 2021). A new burnishing tool has been developed to perform the fine surface finish of a hardened stainless steel in (Shiou et al. 2017). The effect of roller burnishing and slide roller burnishing on surface integrity of AISI 316 steel has been investigated in (Maximov et al. 2024). The burnishing of a non-axisymmetric curved surface with a CNC lathe has been presented in (Takasugi et al. 2021). An investigation into ball burnishing process of magnesium alloy on CNC lathe using different environments has been carried out in (Cagan et al. 2020). A sequential ball grinding, ball burnishing and ball polishing processes have been developed in (Shiou et al. 2008), to improve the surface roughness of the stainless tool steel, whereas a slurry container or slurry circulation system was needed. There is no polishing device has been developed to be integrated with a CNC lathe to perform the surface finish after a workpiece has been turned or has been burnished.

The objective of this work is to develop a new polishing tool integrated with a CNC turning center and no slurry container is required by using new lab-made polishing balls embedded with abrasives. The design and fabrication of a new ball polishing tool implanted with a load cell for a CNC lathe, the development of the lab-made rubber-based polishing balls embedded with the abrasive of aluminum oxide, the property of the adopted material STAVAX stainless mold steel, and the experimental setup of the ball polishing system on a CNC turning center are introduced in Section 2. The experimental results on the measured surface roughness of the hexagonal surfaces using different types of polishing balls, the volumetric wear of the lab-made polishing balls, the effects of different passes on the surface roughness improvement, and the application to the surface finishing of a cylindrical part with a keyway are reported in Section 3. Some discussions on the effects of different passes on the surface roughness improvement and the future work have been presented in section 4. The main results of this study are summarized in conclusion.

EXPERIMENTAL WORK AND METHODOLOGY

Design of a New Ball Polishing Tool Embedded with a Load Cell

To improve the surface roughness of the fine turned and burnished workpiece, a new ball polishing tool primary including an electrical grinder and a load cell, has been designed and manufactured in this research. The design consideration was based on the development of the burnishing tool used in a CNC lathe (Shiou et al. 2017).

The new ball polishing tool has been designed, as shown in Figure 1. The polishing tool mainly comprises of a VDI 30 tool adapter, a tool holder, a load cell, a mold helical spring, a cover with a safety screw, a holder for an electrical grinder, an electric grinder, and a polishing ball. The VDI 30 tool adapter can be mounted on the VDI tool holder of the turret of a CNC lathe. A mold helical spring with the spring constant of 15.0 N/mm was used to absorb the vibration of the machine bed and the positioning error of the CNC lathe. Two spring retainers were used to guide the movement of the mold spring and transmit the polishing force to the load cell. A U-slot was milled in the inner cover body to limit the movement of the spring, to protect the load cell, and to work as a safety device. A lab-made polishing ball can be mounted on the electric grinder. The load cell embedded in the polishing tool is a product of the Honeywell Company, model 53 (Load cell 2024). The maximum loading for the adopted load cell was about 111 N.

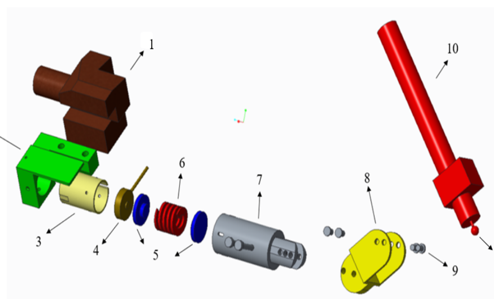

1. VDI30 adapter 2. Tool holder 3. Inner cover 4. Load cell 5. Spring retainers 6. Mold spring 7. Outer cover 8. Holder of electrical grinder 9. Screws 10. Electrical grinder 11. Polishing ball.

Fig. 1. Exploded view of the ball polishing tool embedded with a load cell

Integration of the Polishing Tool with the CNC Turning Center

Figure 2 shows the developed polishing tool mounted on the 3-axis CNC turning-milling center, type YLM8A equipped with a FANUC-0i-TD controller. The 3-axis (X-Z-C) CNC turning-milling center is equipped with a power turret with 12 tool holders. The resolution of the C-axis is 0.001°, such that a hexagonal-shaped workpiece could be fabricated by using the NC commands of polar coordinate transformation. The developed polishing tool was mounted on one of the tool holders of the turret. The induced polishing force signal is amplified by an amplifier and emitted by a wireless transmitter, type T24-ACMn-SA. The amplified signal is then received by a receiver embedded with an A/D converter, type T24-BSU, connected to a PC via a USB interface. The NC codes needed for turning, ball burnishing, and ball polishing paths were simulated and generated by the Master CAD/CAM software. After machining path simulation, these generated NC codes can then be transmitted to the CNC controller of the CNC turning-milling center via RS232 serial interface.

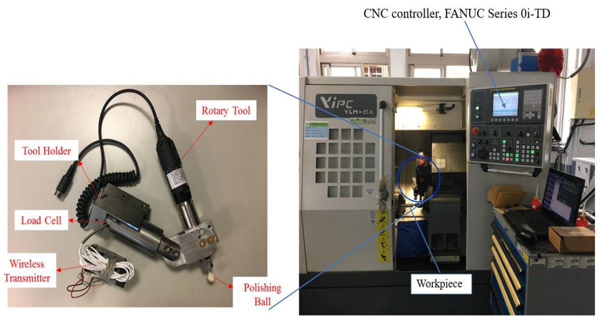

Fig. 2. Integration of the fabricated polishing tool with the 3-axis CNC turning-milling center

Material and Specimen Preparation

The STAVAX stainless mold steel used in this study includes corrosion and wear resistance with excellent properties in polishing, machinability, and stability in hardening (STAVAX ESR 2024). It can be applied to all type of molds and is especially suited for larger tools where corrosion in production is unacceptable and where high surface finish is required. Table 1 shows the chemical composition of the STAVAX stainless mold steel we used. The hardness of this material is about HRC20 after tempering.

Table 1. Chemical composition of STAVAX stainless steel (%) (STAVAX ESR 2024).

Composition	C	Si	Mn	Cr	V
%	0.38	0.9	0.5	13.6	0.3

Using an end mill mounted on a power turret, a hexagonal-shaped STAVAX specimens fine milled from a cylinder with a diameter of 38 mm have been designed, fine turned and milled, directly on the CNC turning center so that the sequential ball burnishing and ball polishing on each of the hexagonal surface could be carried out. Each type of the lab-made polishing balls, type A to E, has been applied to do the ball polishing after the ball burnishing on the hexagonal surface, as shown in Figure 3. The area of the specimen to be burnished and polished were 10 x 5 mm, separately.

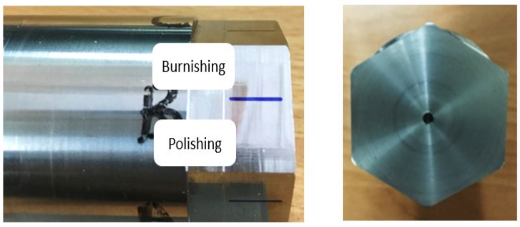

Fig. 3. Ball burnishing and ball polishing on a hexagon-shaped STAVAX specimen.

Development of the Lab-made Polishing Balls Embedded with the Abrasive of Aluminum Oxide

Considering the slurry container no longer being used, a new polishing balls embedded with abrasives has been developed in this study, such that a slurry circulation system will not be used. The abrasive of aluminum oxide (Al_2O_3) is suitable for polishing the stainless mold steel, according to the previous study results (Shiou et al. 2022). As a result, a new polishing ball embedded with abrasive of aluminum oxide has been developed by taking the Nitrile Butadiene Rubber (NBR) as matrix, mixing with the abrasive of aluminum oxide with different sizes (0.05 um to 3 um) and concentration and the additives of Silicon Oxide, as indicated in Table 2. Concerning the good physical, mechanical, and chemical properties, such as abrasion resistance, adhesion to metal, compression set, tear resistance, vibration dampening, and solvent resistance, etc., the NBR has been selected as the matrix material. Five type of polishing balls NBR-based blanks has been made after the NBR, abrasives and some additives have been homogenously mixed by a blending machine. The hardness of each blank has been tested by using the Shore hardness tester. After the tensile test specimens have made from the NBR-based blanks, the yielding strength and the static coefficient of friction have been tested by using a universal material testing machine. The measured results of the hardness, yielding strength, and the static coefficient of friction have been summarized in Table 2. To verify the chemical composition of the NBR-based blanks, different types of the blanks have been inspected by the scanning electron microscope (SEM) and energy-dispersive X-ray spectroscopy (EDS). Figure 4 shows the graphs of SEM and EDS of Type A blank with the abrasive size of 0.05 µm and concentration of 20%, observed with the magnification ratio of 25,000. The abrasive of aluminum oxide (Al_2O_3) and silicon oxide could be observed by the EDS. The graphs of SEM and EDS of Type B polishing ball (0.3 µm, 20%) with the magnification ratio of 15,000 are shown in Figure 5. Figure 6 shows the graphs of SEM and EDS of Type C blank with the abrasive size of 1.00 µm and concentration of 30%, observed with the magnification ratio of 2,000. The graphs of SEM and EDS of Type D polishing ball (3 µm, 20%) with the magnification ratio of 350 are shown in Figure 7. Figure 8 shows the graphs of SEM and EDS of Type E polishing ball (3 µm, 40%) with the magnification ratio of 350.

Table 2. Concentration and abrasive size of aluminum oxide (Al_2O_3)

Type	A	B	C	D	E
abrasive size (µm)	0.05 µm	0.3 µm	1 µm	3 µm	3 µm
Concentration (%)	20%	20%	30%	20%	40%
Hardness (HAS)	65 HAS	63 HAS	66 HAS	64 HAS	66 HAS
Yielding strength (N/mm^2)	9.516 N/mm^2	8.07 N/mm^2	9.68 N/mm^2	6.84 N/mm^2	10.67 N/mm^2
Static coefficient of friction	0.98	0.96	0.74	0.61	0.6

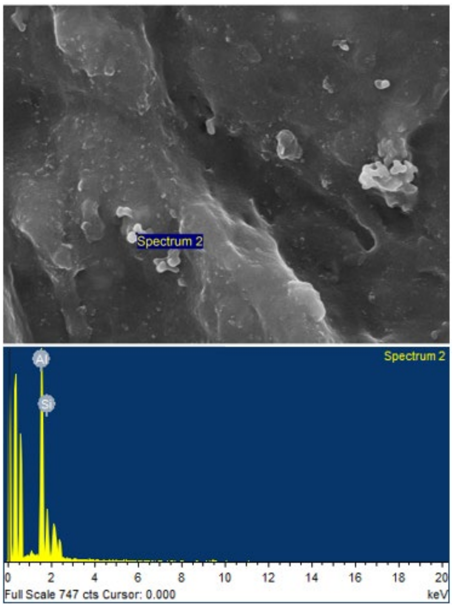

Fig. 4. SEM and EDS of Type A polishing ball (0.05 µm, 20%) with the magnification ratio of 25,000

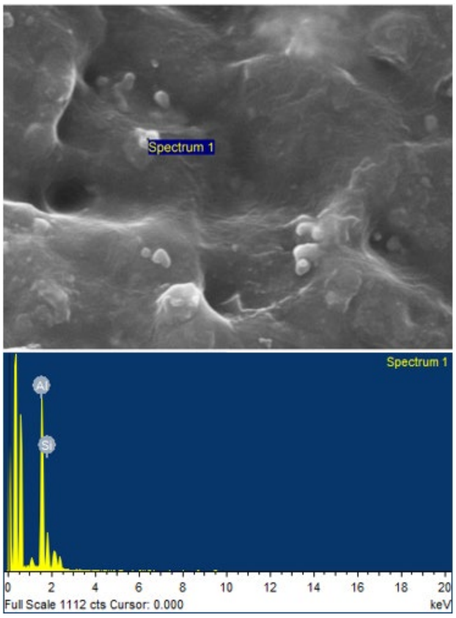

Fig. 5. SEM and EDS of Type B polishing ball (0.3 µm, 20%) with the magnification ratio of 15,000

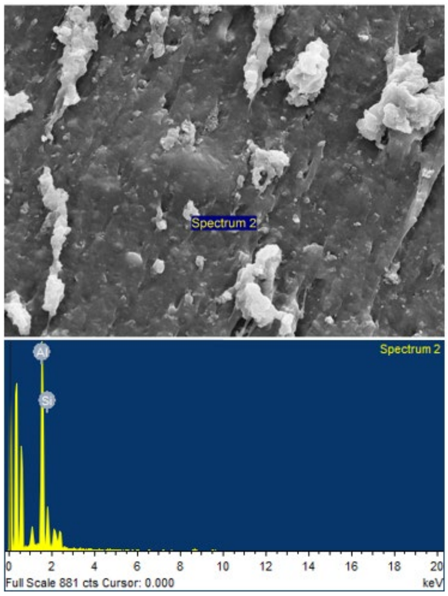

Fig. 6. SEM and EDS of Type C polishing ball (1 µm, 30%) with the magnification ratio of 2000

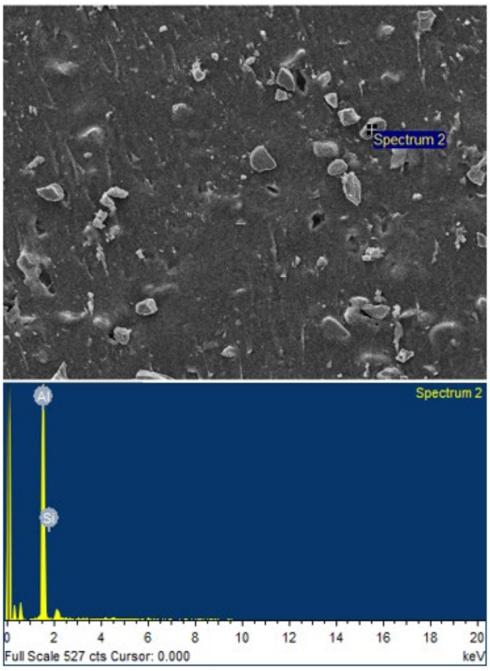

Fig. 7. SEM and EDS of Type D polishing ball (3 μm, 20%) with the magnification ratio of 350

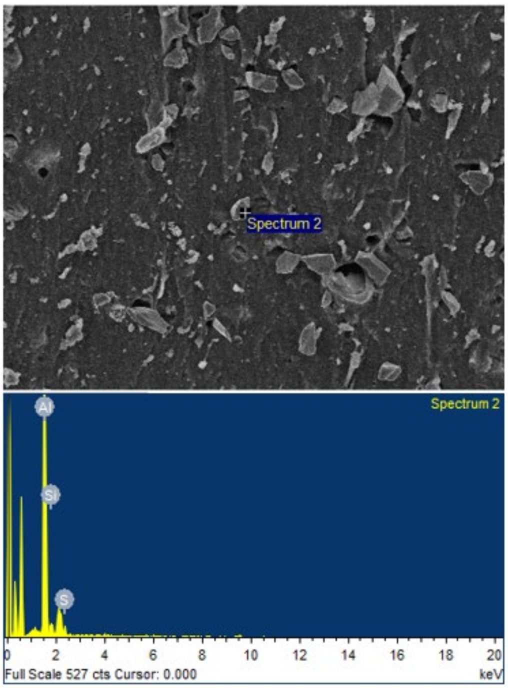

Fig. 8. SEM and EDS of Type E polishing ball (3 μm, 40%) with the magnification ratio of 350

A mold made of Al-6061T6 with the hardness of HRB 54 has been designed and fabricated to fabricate the polishing balls. Different kinds of polishing balls with the diameter of 12 mm have been fabricated by the thermal forming processes, as shown in Figure 9.

Fig. 9. Photo of the fabricated lab-made polishing balls.

Use of Suitable Ball Burnishing and Ball Polishing Parameters

The sequential fine turning, milling, ball burnishing, and ball polishing processes were adopted in this study for the surface finishing of the specimens and test carrier. Table 3 listed the suitable combination of the ball burnishing parameters for the STAVAX specimen, based on the research results in (Shiou et al. 2017). The burnished surfaces on the hexagonal surfaces have been furthered polished by using the lab-made polishing balls. The suitable combination of the ball polishing parameters for the specimen, referred to the previous study in (Shiou et al. 2022), has been summarized in Table 4.

Table 3. Combination of the suitable ball burnishing parameters

Factors	Parameter
Ball material	WC
Ball Diameter(mm)	8
Burnishing Force(N)	110
Feed(mm/rev)	0.05
Spindle Speed(rpm)	235
Emulsion lubricant (Oil : Water)	1:20
No. of Passes	1

Table 4. Combination of the suitable ball polishing parameters

Factors	Parameter
Ball Material	NBR embedded with Al_2O_3
Diameter (mm)	12
Depth of Penetration (μm)	180
Feed (mm/rev)	0.02
Spindle Speed (rpm)	5000
Lubricant (Oil: Water)	1:20
No. of Passes	1

RESULTS AND DISCUSSION

Measured Surface Roughness of the Hexagonal Surfaces Using Different Types of Polishing Balls

The Hommelwerke T8000 roughness and contour tester, made by JENOPTIC (Jena, Germany), was used to measure the surface roughness of the fine-turned, fine-milled, burnished, and polished specimens. The surface roughness of the fine-turned specimen was about Ra 0.21 um. After the sequential fine milling and ball burnishing, five types of the lab-made polishing balls have been applied to the five the hexagonal surfaces. The polishing time for the area of 10 x 5 mm was about 15 minutes by fixing the feed rate of 60 mm/min and stepover of 50 microns. The measured average surface roughness values from three measurements have been listed in Table 5. The surface roughness was improved from 0.22 um to about 0.11 um after ball burnishing on average. The surface roughness improvement ranges from 0.077 um (Type A) to 0.046 um (Type E) on average after ball polishing. In general, the greater the grain size (3um) of the abrasive, the more the improvement (0.06um) on the surface roughness.

Table 5. Surface roughness of the fine-milled, burnished, and polished surfaces using different types of polishing balls.

Process	Type A	Type B	Type C	Type D	Type E
Fine milling (Ra)	0.22 μm	0.22 μm	0.22 μm	0.22 μm	0.22 μm
Ball burnishing (Ra)	0.113 μm	0.116 μm	0.113 μm	0.11 μm	0.106 μm
Ball polishing (Ra)	0.077 μm	0.073 μm	0.06 μm	0.056 μm	0.046 μm
Improvement on ball polishing	0.036 μm	0.042 μm	0.053 μm	0.054 μm	0.06 μm

Volumetric Wear of the Lab-made Polishing Balls

To evaluate the volumetric wear of the lab-made polishing balls from type A to type E, a solid model of the used polishing balls was constructed using a coordinate measuring machine to measure the profile of the polishing ball with wear. The Creo parametric software has been used to construct the 3D solid model. The constructed solid models are shown in Figure 10 (a), (b), (c), (d), and (e), respectively. It shows that the volumetric wear of the polishing balls ranges from 1.1% (type A) to 5.7 % (type E), as shown in Table 6. The volumetric wear is increasing with the increase of the gran size and the concentration of the abrasives. The possible reason for that is the surface total bounding area decrease when the increase of the gran size and the concentration of the abrasives.

(a) (b) (c) (d) (e)

Fig. 10. Constructed CAD model of the volumetric wear of the lab-made polishing balls (a) Type A (b) Type B (c) Type C (d) Type D (e) Type E.

Table 6. Volumetric wear of different types of the polishing balls

Dimension	Type A	Type B	Type C	Type D	Type E
Diameter	11.80 mm	11.76 mm	11.78 mm	11.72 mm	11.70 mm
Volume	860.29 mm^3	851.57 mm^3	855.92 mm^3	840.91 mm^3	838.60 mm^3
Wear volume	9.70 mm^3	27.22 mm^3	20.91 mm^3	46.37 mm^3	47.98 mm^3
Ratio	1.10%	3.10%	2.50%	5.51%	5.72%

Effects of Different Passes on the Surface Roughness Improvement

To achieve the final surface finish for a precision mold with freeform surface, in general, many polishing passes are needed to improve the surface roughness by reducing the grain size of the abrasives step by step. As a result, the effects of different number of passes on the surface roughness improvement for the lab-made polishing balls have been investigated in this study. Four kinds of passes, namely, Type E-D-C-B-A, Type E-C-B-A, Type E-B-A, and Type E-A, has been figured out and tested, by reducing the grain size of the abrasives sequentially, as shown in Table 7. According to the experimental results, the more the number of the polishing passes, the better surface roughness could be obtained. However, the more the number of polishing passes is performed, the more the polishing time is required. About 15 minutes was needed for each additional polishing path. The burnished surface with a surface roughness of Ra 0.11um could be improved to 0.023 um using the type E-D-C-B-A passes and the type E-C-B-A passes, individually. The possible reason that the type E-D-C-B-A and type E-C-B-A have the same AVG(Ra) value 0.023um after polishing, is that both the type D and type E have the same abrasive size of 3 um and with different abrasive concentration. The influence of pass D on the surface roughness improvement was not obvious. To reduce the polishing time about 15 min. and to obtain a good surface roughness of Ra 0.023 um, the type E-C-B-A is suggested to be used. Utilizing the Type E-A passes, the surface roughness of Ra 0.04 um was achievable.

Table 7. Comparison of different number of the passes of ball polishing on the surface roughness

No. of Pass	Test 1(R_a)	Test 2(R_a)	Test 3(R_a)	AVG. (R_a)
Type E-D-C-B-A	0.02 μm	0.02 μm	0.03 μm	0.023 μm
Type E-C-B-A	0.02 μm	0.03 μm	0.02 μm	0.023 μm
Type E-B-A	0.04 μm	0.03 μm	0.03 μm	0.033 μm
Type E-A	0.04 μm	0.04 μm	0.04 μm	0.04 μm

Application of the Pass Type E-C-B-A to the Surface Finishing of a Cylindrical Part with a Keyway and a Test Carrier with a Cam Profile

A cylindrical part with a keyway has been designed as a test carrier, as shown in Figure 11(a). By using an end mill mounted on a power turret, the keyway has been milled after the fine turning process directly on the CNC turning-milling center. The ball burnishing process has been carried out after the fine milling process. The developed new polishing tool, the lab-made polishing balls, and the ball polishing have been sequentially applied to the burnished surface of the test carrier. The surface roughness R_a of the surface region on the tempered STAVAX tested part, can be improved sequentially from about 0.21 µm to 0.02 µm, as shown in Figure 11(b). The surface roughness value Ra on the burnished surface was 0.11µm on average. The surface roughness value Ra on the ball polished surface was 0.02 µm, as shown in Figure 12. The surface roughness improvement of the tested object on the burnished surface was about 48%, and that on the ball polished surface using the suggested E-C-B-A passes was about 82%.

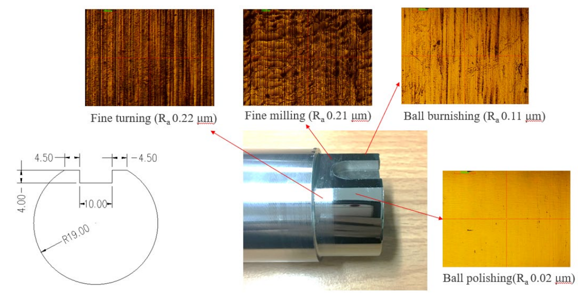

(a) (b)

Fig. 11. Surface finishing of a cylindrical part with a keyway (a) cross section of the test carrier (b) surface textures on the fine turned, milled, burnished, and polished surfaces.

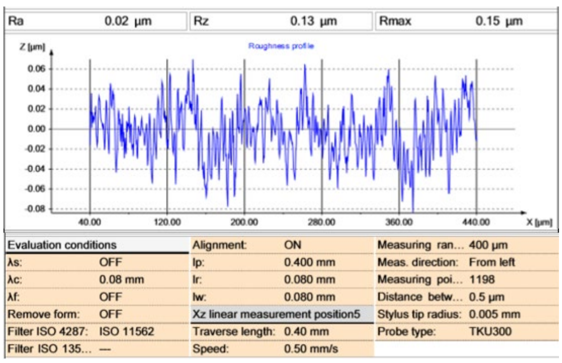

Fig. 12. Measured surface roughness of the polished area of test carrier.

A test carrier with a cam profile has been designed as a test carrier, as shown in Fig 13. The workpiece has been turned and milled sequentially on the CNC turning-milling center. The ball burnishing process has been carried out after the fine milling process. The developed polishing tool with the lab-made polishing balls has been applied to the burnished surface of the test carrier. The surface roughness R_a of the fine milled surface, can be improved sequentially from about 0.21 µm to 0.023 µm on average, as shown in Figure 13. The surface roughness value Ra on the burnished surface was 0.106µm on average. The surface roughness value Ra on the ball polished surface was 0.023 µm on average, as shown in Table 8. The surface roughness improvement of the tested object on the burnished surface was about 48%, and that on the ball polished surface using the proposed E-C-B-A passes was about 82%.

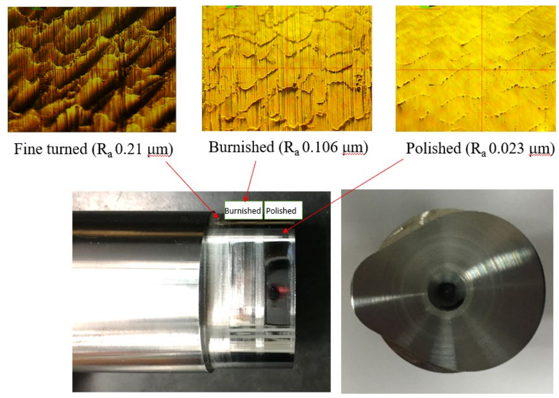

Fig. 13. Photo of the polished test carrier with a cam profile

Table 8 Measured surface roughness of the test carrier with a cam profile

Process	Test 1(R_a)	Test 2(R_a)	Test 3(R_a)	AVG. (R_a)
Fine milling	0.20 µm	0.21 µm	0.22 µm	0.21 µm
Ball burnishing	0.12 µm	0.11 µm	0.09 µm	0.106 µm
Ball polishing	0.02 µm	0.03 µm	0.02 µm	0.023 µm

Discussion

Despite the new polishing tool and the lab-made polishing balls have been presented, there are still some issues to be discussed and investigated in the future. Based on the experimental results of the different number of the passes of ball polishing on the surface roughness improvement, the Type E-D-C-B-A and Type E-C-B-A had almost the same result. It implied that the variation of the concentration of the abrasive with same grain size had no obvious influence on the surface roughness improvement. To eliminate the polishing time, the number of the passes Type E-B-A or E-A could be considered, concerning the polishing time of one pass for the area of 10 x 5 mm was about 15 minutes. Polishing using the Type E-B-A or Type E-A may reduce the polishing time of 15 to 30 minutes. The constant force polishing process is suggested to be implemented, concerning the wear of the polishing ball. Different kind of diameters of the polishing balls instead of 12 mms could be designed and fabricated, to adapt the diameter of the workpiece.

CONCLUSION

A new ball polishing tool that can be mounted on the turret of a CNC turning center, and the lab-made polishing balls have been developed in this work, to perform the ultraprecision surface finish of the STAVAX mold steel. The new ball polishing tool, including an electric grinder and embedded with a load cell, has been designed and fabricated. The polishing tool can be mounted on a VDI tool holder of the turret of a CNC turning-milling center, such that the automated surface finishing is possible.

Five types of polishing balls with different abrasive grain sizes and concentration, from type A to type E, have been figured out, fabricated, and tested. Based on the experimental results on the hexahedron surfaces as the test specimens, the type E polishing ball (particle size of 3 μm, concentration of 40%) has the best surface roughness improvement value of Ra 0.046 μm. The volumetric wear of the lab-made polishing balls from type A to type E has been evaluated by constructing a 3D solid model of the used polishing balls. In general, the volumetric wear is increasing with the increase of the gran size and the concentration of the abrasives.

The effects of different passes on the surface roughness improvement for the lab-made polishing balls, namely, type E-D-C-B-A, type E-C-B-A, type E-B-A, and type E-A, has been investigated in this study. The type E-C-B-A is suggested to be used, to reduce the polishing time and obtain a good surface roughness of Ra 0.023 um. The proposed new polishing tool has been applied to the test carrier with a keyway using the suitable parameters in ultra-precision manufacturing. The surface roughness of the test carrier could be improved form Ra 0.206 μm to Ra 0.02 μm. The proposed device is potentially useful in different nonconventional and hybrid manufacturing platforms.

ACKNOWLEDGMENT

This research has been sponsored by the Ministry of Science and Technology of the Republic of China (Taiwan) under grant NSTC 112-2221-E-011-097.

REFERENCES

Bae, J.T. and Kim, H.J., "Finishing characteristics of Inconel alloy 625 bars in ultra-precision magnetic abrasive finishing using CNC machine center", *J. Mech. Sci. Technol.,* Vol. 35 pp. 2851-2859 (2021).

Cagan, S.C., Pruncu, C.I. and Buldum, B.B., "An investigation into ball burnishing process of magnesium alloy on CNC lathe using different environments", *J. Magnes. Alloy.* Vol. 8, pp. 1061-1070 (2020).

Cao, C., Zhu, J., Tanaka, T., Shiou, F.J., Sawada, S. and Yoshioka, H. "Ball burnishing of Mg alloy using a newly developed burnishing tool with on-machine force control", *Int. J. Automot. Technol.*, Vol. 13, pp. 619–630 (2019).

Ganesan, G., Malayath, G. and Mote, R.G. "A review of cutting tools for ultra-precision machining", *Mach. Sci. Technol.,* Article in Press (2023).

Hatefi, S. and Abou-El-Hossein, K., "Experimental investigation on the effects of magnetic field assistance on the quality of surface finish for sustainable manufacturing of ultra-precision single-point diamond turning of titanium alloys", *Front. Mech. Eng.,* Vol. 8, (2022).

Kasuriya, P., Watanabe, T., Goto, T. and Jin, M. "Mirror surface finishing of hardened stainless steel using spherical PCD tool", *Precis. Eng.*, Vol. 74, pp. 163-174 (2022).

Load Cells. Available on https://prod-edam.honeywell.com/content/dam/honeywell-edam/sps/siot/en-us/products/test-and-measurement-products/load-cells/common/documents/sps-siot-testest-and-measurementeasurement-load-cell-range-guide-008886-2-en-ciid-150503.pdf?download=false (2024)

Lou Y. and Wu H., "Effect of parameters on surface roughness during the ultra-precision polishing of titanium alloy using bonnet polishing", *PLoS One*. Vol. 17 (2022).

Maximov, J., Duncheva, G., Anchev, A., Dunchev, V., Anastasov, K. and Daskalova, P., "Effect of Roller Burnishing and Slide Roller Burnishing on Surface Integrity of AISI 316 Steel: Theoretical and Experimental Comparative Analysis", *J. Machines.*, Vol. 12, No. 51 (2024).

Micallef, C., Zhuk, Y. and Aria, A.I., "Surface finishing and tool wear in single point diamond turning of chemical vapour deposited tungsten carbide hard coatings", *Surf. Coat. Technol.,* Vol. 447(2022).

Shiou, F.J., Huang, S.J., Shih, A.J., Zhu, J. and Yoshino, M., "Fine Surface Finish of a Hardened Stainless Steel Using a New Burnishing Tool", *Procedia Manuf.* Vol. 10, pp. 208-217 (2017).

Shiou, F.J. and Hsu, C.C., "Surface finishing of hardened and tempered stainless tool steel using sequential ball grinding, ball burnishing and ball polishing processes on a machining centre", *J. Mater. Process. Technol.* Vol. 205, pp. 249–258 (2008).

Shiou, F.J. and Tsegaw, A.A., "Ultra precision surface finishing processes", *Int. J. Automat.*

Technol., Vol. 13, pp. 174–184 (2019).
STAVAX ESR. Available online: https://www.assab.com/app/uploads/sites/133/2020/04/Stavax_ESR_PH-EN.pdf (2023).
Takasugi, K., Shinya, M., Isozaki, Y., Suzuki, N., Kaneko, Y., Asakawa, N. and Morimoto, Y. "Burnishing of a non-axisymmetric curved surface with a CNC lathe", *J. Adv. Mech. Des., Syst. Manuf.* Vol. 15 (2021).
Wu, W., Shi, C., Li, K., Yu, Y., Wang, T., Zhong, B., Wang, Z., Guo, J., Cheung, C.F. and Wang, C., "The theoretical and experimental investigation of material removal in semi-rigid bonnet polishing of binderless tungsten carbide", *J. Mater. Res. Technol.*, Vol. 24, pp. 1597-1611 (2023).
Wu, Z., Shen J., Peng Y. and Wu, X., "Review on ultra-precision bonnet polishing technology", *Int. J. Adv. Manuf. Technol.*, Vol. 121, pp. 2901–2921 (2022).

於 CNC 切削中心機使用新型球拋光工具進行不銹鋼之表面精加工

修芳仲 洪詩函 黃偉誠
國立台灣科技大學機械工程系

吳昌謀
國立台灣科技大學材料與工程工程系

摘 要

本研究主要探討開發一新型球拋光工具並使用自製拋光球整合於 CNC 車銑複合機對 STAVAX 模具不鏽鋼進行表面精加工之研究。表面精加工之參數使用先期研究之最佳球擠光、球拋光加工參數組合，探討本研究研製五種型號之自製拋光球對表面粗糙度影響，最後將最佳參數組合應用於車銑複合製造出的試件。本研究經由六面形作為試件的實驗結果得到 Type E(磨料粒徑 3 μm，濃度 40%)拋光球對表面粗糙度改善值最高；本研究也探討拋光道次對表面精加工的影響，經實驗結果可得最佳球拋光順序與道次組合為：Type E(磨料粒徑 3 μm，濃度 40%) - Type C(磨料粒徑 1 μm，濃度 30%) - Type B(磨料粒徑 0.3 μm，濃度 20%) - Type A(磨料粒徑 0.05 μm，濃度 20%)，可使表面粗糙度由 Ra 0.22 μm 改善至 Ra 0.023 μm。本研究以六面形作為實驗試件所獲得最佳球擠光、球拋光順序與道次參數組合應用於車銑複合工具機製造出的凸輪、具鍵槽試件進行加工，拋光後凸輪與具鍵槽試件表面粗糙度分別由 Ra 0.21 μm 改善至 Ra 0.023 μm 及 Ra 0. 206 μm 改善至 Ra 0.02 μm。